Assessment of Anterior Spinal Artery Blood Flow following Spinal Cord Injury

Mohammed Alshareef[1], Ahmed Alshareef[2], Vibhor Krishna, M.D.[3], Mark Kindy, Ph.D.[3], and Tarek Shazly, Ph.D[4,*]

[1]College of Medicine, Medical University of South Carolina, Charleston, SC, [2]Department of Biomedical Engineering, Duke University, Durham, NC, [3]Department of Neurosurgery, Medical University of South Carolina, Charleston, SC, [4]Department of Mechanical Engineering, University of South Carolina, Columbia, SC

*Corresponding author: 300 Main Street, Columbia, SC 29208, Shazly@cec.sc.edu

Abstract

The incidence of spinal cord injury (SCI) in the US is approximately 12,000 individuals annually, due to various forms of trauma and disease. (1) Previous studies show that increased force on or prolonged compression of the spinal cord results in progressive ischemia, as indicated by a reduction in spinal cord perfusion (3). Diminished flow over a prolonged period of time can cause necrosis and permanent damage if perfusion falls below the critical level, or vascular threshold (4). We constructed a 3D finite element model of the cervical spinal cord to examine the role of compressive mechanical loading of the spinal cord on blood flow and ischemia, which could arise from acute compression, distraction, or vasospasms. It was found that the magnitude and direction of forces on the spinal cord model, including anterior, posterior, and axial loading, had distinct effects on blood flow. Maximal reduction in perfusion was shown in the posterior loading, while maximal reduction in flow of the anterior spinal artery was shown in the anterior loading. Changes in the mechanical properties of the spinal cord showed slight reduction in blood flow rate. Therefore, this study provides evidence that spinal damage at subclinical thresholds creates a decrease in blood flow that could progress into ischemia and makes the spinal cord susceptible to further damage.

Keywords: anterior spinal artery, spinal cord injury, blood flow, fluid-structure interaction

1. Introduction

The incidence of spinal cord injury (SCI) in the US is approximately 12,000 individuals annually, due to various forms of physical applied loads. (1) Often times, compression of the spinal cord occurs and remains past the initial impact of the injury. Multiple studies have been conducted to study the relationship between initial severity of compression and recovery. (2,3,4) An injury threshold was identified, above which there is no return of functionality. (5,6) Alternatively, it was also shown that compressions causing <35% canal stenosis were clinically negligible, with no presentable symptoms. (7) The results of these studies were acquired by direct examination of the study of animals and their post-decompression functionality. Other studies have analyzed compression by measurement of the somatosensory evoked potentials. (8) To our knowledge, no studies have shown the relationship between spinal compression and spinal vascular mechanics at subclinical compressive loading, specifically ones causing >35% canal stenosis.

Spinal compression is typically the combined result of primary and secondary spinal cord injury. Secondary injury mechanism, believed to occur through an inflammatory response from the host, causes further injury past initial trauma (9). Primary injury, including impact and acute compression, in addition to secondary injury mechanisms produces progressive spinal cord ischemia (10). Experimental results show that increased force on or prolonged compression of the spinal cord results in progressive ischemia, as experimentally determined by spinal cord perfusion (9). This progressive decline over a prolonged period of time can cause necrosis and permanent damage if perfusion falls below the critical level, or vascular threshold. (7) Ischemia, thus, must be treated in a time-sensitive matter, and evidence shows that immediate treatment can restore spinal cord function. (11)

Treatment of ischemia caused by primary and secondary SCI requires knowledge of the causes of the reduced blood flow. While there are several hypotheses including vasospasms due to mechanical damage (12, 13), endothelial damage or swelling (14,

Excerpt from the Proceedings of the 2012 COMSOL Conference in Boston

15, 16), and thrombosis (17), to suggest ischemic consequences of SCI, the exact cause of posttraumatic ischemia is not well defined (9). This paper examines the role of compressive mechanical loading on ischemia, which could arise from a number of primary and secondary injury mechanisms, including acute compression, distraction, or vasospasms. A finite element model (FEM) with the spinal cord and dura mater was constructed using Comsol to study the effects of different loading scenarios on the blood flow in the anterior spinal artery. Parametric studies were performed to establish a qualitative relationship between relatively small displacements and reduction in percent blood flow. We predict a change in blood flow that would additively account for a significant reduction in perfusion. Furthermore, studies have shown a reduction in the spinal cord elastic modulus as a result of tissue degeneration and necrosis (28). We hypothesize a reduction in blood flow due to a decrease in the spinal cord elastic modulus, which would amplify the damage caused by the initial compression.

2. Use of COMSOL Multiphysics

A 3D FEM model of the cervical spinal cord was developed using Comsol Multiphysics 4.0a. The fluid-structure interaction physics module was used to study blood flow-spinal cord interaction. The model included a 1 cm segment of the spinal cord, surrounding dura mater, the anterior spinal artery, and 5 arterial branches that protrude into the spinal cord, as shown in Figure 1. The size of the arterial branches was selected at 100 μm with a wall thickness of 80 μm and sub-branches were assumed absent. Velocity through the arterial branches was measured at approximately 10 mm/s. The ASA was defined as a 1.4 mm vessel with 0.2 mm thickness and a flow velocity of approximately 0.3 m/s. All solid materials in the model were characterized as linear elastic with their properties and geometries cited from literature in table 1.

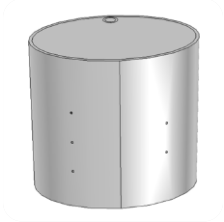

Figure 1: Cervical spine model with (from deep to superficial) anterior spinal artery, spinal cord, and dura mater. The five arterial branches were allowed to leave the dura mater for analysis and simulate blood flow out of the spinal cord

2.2 Fluid Flow

Blood was modeled as a Newtonian fluid with a density of $\rho = 1060$ kg/m^3 and a dynamic viscosity, μ =5e-3 Pa.s. Boundary conditions were automatically applied to the entire geometry by the software. Blood flow was induced by a pressure gradient of 2000 Pa. The areas of the inlet and outlet were fixed to allow for consistent flow rate readings with changes in velocity. The outlet and inlet flows were quantified as a result of the applied compressions. Flow was also quantified as a result of changes in the mechanical properties of the spinal cord and the anterior spinal artery. Blood was modeled as a laminar Newtonian fluid was single-phased flow based on the Navier-Stokes equation. Furthermore, the fluid was assumed to be under incompressible flow. Finally, adaptive meshing was applied to the geometric volume using tetrahedral elements.

2.3 Structural Mechanics

Each solid was modeled as a linear elastic material with a total strain tensor written in the form of a displacement gradient. The Young's modulus and Poisson's ratio of each material were given as shown in table 1. The software implemented solid conditions based on the stress and strain variables.

2.4 Experimental loadings and conditions

The loads were defined as the total force (N) applied on each boundary, or face of the 3D model. The software divides the given force by the area of the boundary, giving force per area (N/m^2). The fluid-solid interface boundary condition was set up by the software to define fluid load on the structure and how structural displacements may alter flow velocity. The flow rate was calculated by the integration of the velocity magnitude across the inlet and outlet areas, which were kept constant.

Loads were applied anteriorly, posteriorly, and axially (along the spinal cord), simulating the most clinically applicable types of injuries. Figure 2 shows the boundaries on which forces were applied in each loading scenario. The displacement caused by different loading scenarios was tested to quantify stenosis caused in mm. The mechanical properties of the spinal cord and ASA were also tested by applying a constant 25 N load and measuring flow rate as a function of the elastic modulus of each component.

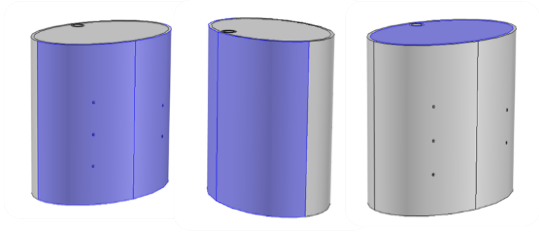

Figure 2: From Left to right: posterior loading, anterior loading, axial loading

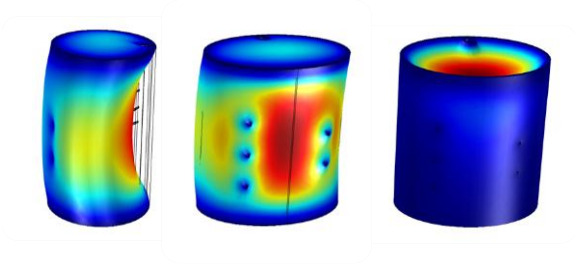

Figure 3: Left to right: anterior loading, posterior loading, axial loading under static loading conditions.

3. Results

Figure 3 shows the loadings anteriorly, posteriorly, and axially with visible displacement on the spinal cord. As shown in figure 4, anterior loading resulted in an initially cumulative increase of blood flow through the arterial branches, mainly due to an increase in the pressure gradients in the lumen of the ASA. However, flow begins to decrease after increasing to a force corresponding to approximately 0.8mm of deformation due to significant vascular occlusion of blood flow. In contrast, figure 7 shows that the anterior spinal artery underwent 22% reduction with a loading that resulted in up to 1 mm displacement of the spinal cord.

Posterior loading resulted in a more dramatic drop of percent blood flow in the vascular branches, as shown in figure 5. This result was indicative of a drastic fall in perfusion of the spinal cord under this loading scenario. However, the percent flow of blood in the ASA was not affected, thus leaving the anterior spinal blood supply intact, as shown in figure 7.

The effects of axial loading were more diverse than the former loading scenarios. The most affected vascular branches were those in proximity of the loading site, as shown in figure 6. It is notable that branches L1 and R1 underwent a decrease in flow rate that was more significant than the posterior loading. At the level of L1 and R1, the spinal cord may undergo significant ischemia, which affects not only that level but the rest of the spinal cord tracts below. Similarly to posterior loading, axial loading did not significantly affect ASA flow, as shown in figure 7.

The mechanical properties of the spinal cord and ASA were also studied for effects on flow. Figure 8 shows that the reduction of spinal cord elastic modulus caused a maximum reduction of 7% in the branches. The ASA was not as significantly affected by this simulated degradation. As shown in figure 9, the reduction of the ASA elastic modulus did not have a significant impact on flow through the branches, a maximum reduction of approximately 2%.

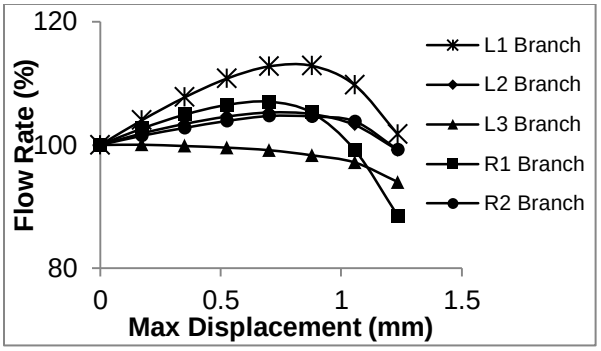

Figure 4: Flow in the vascular branches as a result of anterior compression of the spinal cord

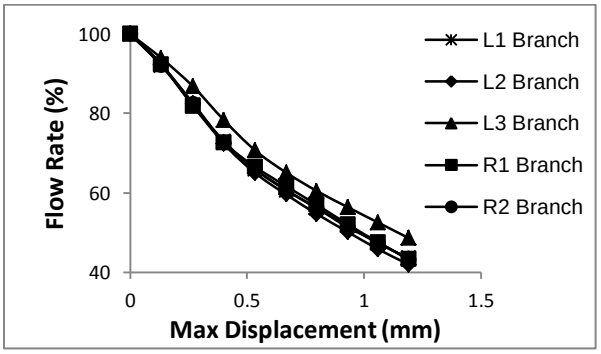

Figure 5: Flow in the vascular branches as a result of posterior compression of the spinal cord

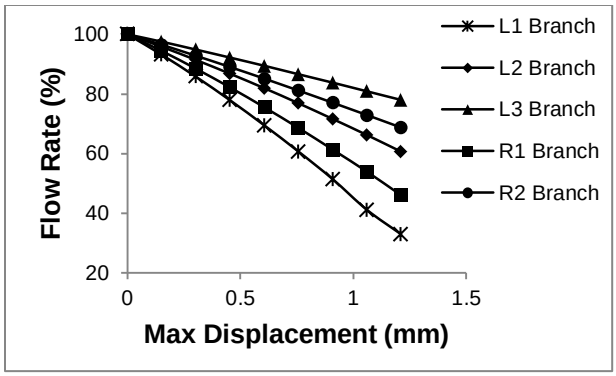

Figure 6: Flow in the vascular branches as a result of axial compression of the spinal cord

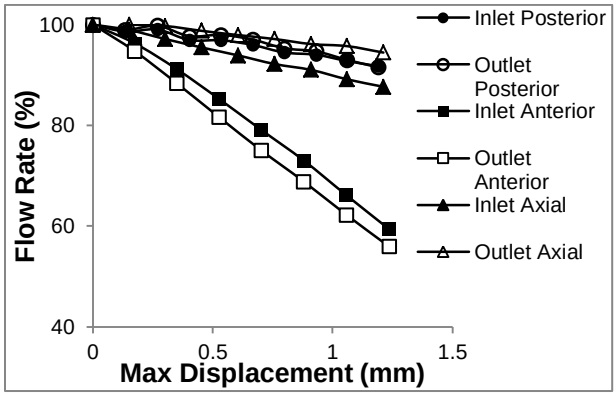

Figure 7: Comparison of percent flow in the ASA as a result of anterior, posterior, and axial compression of the spinal cord

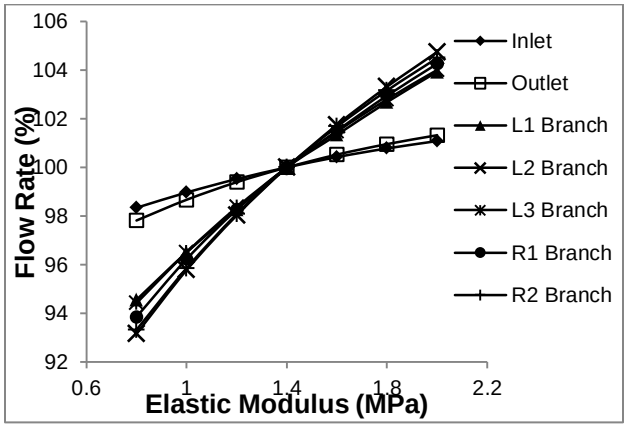

Figure 8: Effects of spinal cord elastic modulus changes on percent blood flow with a constant load of 25N

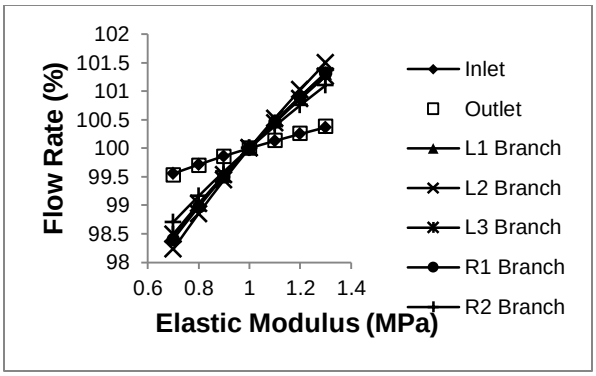

Figure 9: Effects of Arterial wall elastic modulus changes on percent blood flow with a constant load of 25N

4. Discussion

There are some considerable limitations to the spinal cord model associated with the results above. Mechanical damage is not modeled in real-time, as increased and prolonged compression causes deformation and degradation of the spinal cord and its vascular system. Static compression is another limitation because most spinal cord injury are either acute or contain progressive compression. These limitations, however, should not affect qualitative effects of the compressive loadings used. Another limitation is that the spinal cord has a vascular auto-regulation function in response to stress and deformation, but this function cannot be regulated. Furthermore, all of the materials used were modeled as linear elastic materials, which may not accurately describe the mechanical properties of the materials. Since only a 5% deformation is applied, however, the model should still behave accurately with linear elastic behavior. Another limitation is the lack of cerebrospinal fluid (CSF) around the dura mater. This material would not have had an effect on the model because we apply a displacement to the dura mater directly, so the inclusion of the CSF would simply require a greater force to cause such displacement. The model was also limited in its description of blood, chosen as a Newtonian fluid with a steady state flow. This does not accurately describe the response of blood to shear forces in its contact with the lumen of the vessels, as well as its pulsatile state of flow. Finally, there is a limitation in the collateral circulation of the ASA, which has more than one inlet and a more complicated vascular structure, but assuming one inlet and a selected number of vessels still provides an accurate qualitative analysis.

The results gained provide a good understanding of the effects of compressive forces on the vasculature of the spinal cord. The FEM was used to gain insight into the primary determinants of

anterior blood supply under different mechanical loading conditions. Anterior loading results in a notable reduction in ASA flow, which is understood through the significant physical deformation of the artery caused by this mode of compression. We speculate that such a disruption in the configuration of the vessel could compromise the auto-regulation mechanism of the arteries and induce maladaptive remodeling. This loading, however, does not affect the arterial branches as significantly.

Although it minimally affected the ASA, posterior loading reduced perfusion within the spinal cord. It had the greatest effect on the arterial branches. Axial loading did not affect the ASA significantly, but it did affect arterial branches in proximity to loading site, reducing perfusion in branch L1 much more significantly than in L3. Different mechanical properties of the spinal cord were also shown to affect blood flow based on results. Previous studies show that ischemia decreases the elastic modulus of the spinal cord - decreased blood flow caused by spinal compression may be a contributing factor for progressive ischemia and necrosis of the spinal cord.

Although these results do not give us insight into a time frame in which injury to the spinal cord must be dealt with, it does confirm clinical observation in relation to injury. Patients with anterior or axial injury are usually treated based on the severity of injury. Posterior injury patients, however, must be treated in a time-sensitive manner irrelevant of severity, suggesting that the consequences of progressive ischemia are in effect. Future work in this topic would include passive mechanical testing to acquire constitutive equations that more accurately represent the mechanical properties of the vascular system of the spinal cord. Ex-vivo testing of perfusion of fluid through the spinal cord following compressive loads is also of considerable interest.

5. Conclusion

The model was built to assess the involvement of blood flow in different compressions that result from spinal cord injury. We were able to qualitatively analyze the changes in flow and deduced that different directions of loading can result in different types of damage to blood flow. This work will be followed up by a model using constitutive equations for the solid structures involved. We will test the passive and active mechanics of the anterior spinal artery to extract the constitutive equation that dictates its behavior. Finally, this study needs to be replicated by using ex-vivo testing of the various compressions introduced on the spinal cord.

6. References:

1. National Spinal Cord Injury Statistical Center (NSCISC). Spinal Cord Injury Facts and Figures at a Glance. 2010; https://www.nscisc.uab.edu/. Accessed July 10th, 2012.
2. Purdy PD, White CL, 3rd, Baer DL, et al. Percutaneous translumbar spinal cord compression injury in dogs from an angioplasty balloon: MR and histopathologic changes with balloon sizes and compression times. AJNR. American journal of neuroradiology. Sep 2004;25(8):1435-1442.
3. Carlson GD, Gorden CD, Oliff HS, Pillai JJ, LaManna JC. Sustained spinal cord compression: part I: time-dependent effect on long-term pathophysiology. The Journal of bone and joint surgery. American volume. Jan 2003;85-A(1):86-94.
4. Ford RW. A reproducible spinal cord injury model in the cat. Journal of neurosurgery. Aug 1983;59(2):268-275.
5. Croft TJ, Brodkey JS, Nulsen FE. Reversible spinal cord trauma: a model for electrical monitoring of spinal cord function. Journal of neurosurgery. 1972;36(4):402-406.
6. Thienprasit P, Bantli H, Bloedel JR, Chou SN. Effect of delayed local cooling on experimental spinal cord injury. Journal of neurosurgery. Feb 1975;42(2):150-154.
7. Shields CB, Zhang YP, Shields LB, Han Y, Burke DA, Mayer NW. The therapeutic window for spinal cord decompression in a rat spinal cord injury model. Journal of neurosurgery. Spine. Oct 2005;3(4):302-307.
8. Carlson, G. D., C. D. Gorden, et al. (2003). "Sustained spinal cord compression: part I: time-dependent effect on long-term pathophysiology." J Bone Joint Surg Am 85-A(1): 86-94.
9. Tator CH, Fehlings MG. Review of the secondary injury theory of acute spinal cord trauma with emphasis on vascular

mechanisms. Journal of neurosurgery. Jul 1991;75(1):15-26.
10. Ducker TB, Kindt GW, Kempe LG: Pathological findings in acute experimental spinal cord trauma. J Neurosurg 35: 700-708, 1971.
11. Fehlings MG, Tator CH, Linden RD: The effect of nimodipine and dextran on axonal function and blood flow following experimental spinal cord injury. J Neurosurg 71: 403-416, 1989.
12. Doppman JL, Girton M, Popovsky MA: Acute occlusion of the posterior spinal vein: Experimental study in monkeys: J Neurosurg 51 :201-205, 1979.
13. Osterholm JL, Mathews GJ: Altered norepinephrine metabolism following experimental spinal cord injury. Part I: Relationship to hemorrhagic necrosis and post-wounding neurological effects. J Neurosurg 36: 385-394, 1972.
14. Ames A III, Wright RL, Kowada M, et al: Cerebral ischemia. II. The no-reflow phenomenon. Am J pathol 52: 437-453, 1968.
15. Dohrmann GJ, Wagner FC Jr, Bucy PC: The microvasculature in transitory traumatic paraplegia. An electron microscopic study in the monkey. J Neurosurg 35: 263-271, 1971.
16. Fischer EG, Ames A III, Hedley-Whyte ET, et al: Reassessment of cerebral capillary changes in acute global ischemia and their relationship to the “no-reflow phenomenon.” Stroke 8:36-39, 1977.
17. Nemecek S: Morhological evidence of microcirculatory disturbances in experimental spinal cord trauma. Adv Neurol 20: 395-405, 1978.
18. Anatomy of the Spinal Cord . (n.d.). Neuroscience Online. Retrieved July 24, 2012, from http://neuroscience.uth.tmc.edu/s2/chapter03.html
19. Mazuchowski, E. L., & Thibault, L. E. (2003). Biomechanical Properties of the Human Spinal Cord and Pia Mater. Key Biscayne: Summer Bioengineering Conference.
20. hihara, K., Taguchi, T., Shimada, Y., Sakuramoto, I., Kawano, S., & Kawai, S. (2001). Gray matter of the bovine cervical spinal cord is mechanically more rigid and fragile than the white matter. Journal of Neurotrauma, 18(3), 361-367.
21. Nelson SR, Mantz M-L, Maxwell JA (1971) Use of specific gravity in the measurement of cerebral edema. J Appl Physio130: 268 - 271
22. Nelson SR, Mantz M-L, Maxwell JA (1971) Use of specific gravity in the measurement of cerebral edema. J Appl Physio130: 268 - 271
23. Persson, C., Evans, S., Marsh, R., Summers, J., & Hall, R. (2010). Poisson's ratio and strain rate dependency of the constitutive behavior of spinal dura mater.. Ann Biomed Eng., 38(3), 975-83.
24. Persson, C., Summers, J., & Hall, R. M. (2011). The Effect of Cerebrospinal Fluid Thickness on Traumatic Spinal Cord Deformation. Journal of Applied Biomechanics, 27, 330-335.
25. Zhao, S., Logan, L., Schraedley, P., & Rubin, G. (2009). Assessment of the anterior spinal artery and the artery of Adamkiewicz using multi-detector CT angiography. Chinese Medical
26. Torii, R., Oshima, M., Kobayashi, T., Takagi, K., & Tezduyar, T. (2005). Influence of wall elasticity in patient-specific hemodynamic simulations.Computers & Fluids, 36(1), 160-168.
27. Tezduyar, T., Sathe, S., Keedy, R., & Stein, K. (2006). Space–time finite element techniques for computation of fluid–structure interactions. Computer Methods in Applied Mechanics and Engineering, 195(17-18), 2002-2027.
28. Sparrey, C. J., G. T. Manley, et al. (2009). "Effects of white, grey, and pia mater properties on tissue level stresses and strains in the compressed spinal cord." J Neurotrauma 26(4): 585-595.

7. Appendix

Table 1: Material Properties as cited from literature

Material	Size (mm)	Elastic Modulus (Pa)	Poisson's ratio	Density (kg/m^3)	Other
Cervical spinal cord	1-1.5 cm (18)	1.4e6 (19)	0.40 (20)	1050 (21)	
Dura mater	0.3-0.4 (22)	8e7(23)	0.49 (23)	1000 (24)	
Anterior spinal artery	Diameter: 1.5 (25) Thickness: 0.25	1e6 (26)	0.45 (26)	1000 (27)	
Vascular branches	Diameter: 0.1 Thickness: 0.02	1e6	0.45	1000	4.6 branches/cm of spinal cord (18)